Numerical results on a simple model for the confinement of Saturn's F ring

Luis Benet and Àngel Jorba

Abstract In this paper we discuss a simple model for the confinement of Saturn's F ring and present some preliminary numerical results. The model involves the gravitational interaction of independent test particles with Saturn, including its second zonal harmonic, the shepherd moons Prometheus and Pandora, and Titan, the largest of Saturn's satellites. We perform accurate long-time integrations (3.2×10^6 revolutions of Prometheus) to check if the particle has escaped or remains trapped in the region between the shepherds. A particle escapes if its orbit crosses the region between the shepherds, or if it displays a physical collisions (lies with Hill's region) with them. We find a wide region of initial conditions of the test particle that remain confined. We carry out a frequency analysis and use the ratio of the standard deviation over the average main frequencies as stability index. This indicator separates clearly the set of trapped initial conditions of the test particles, displaying some localised structures for the most stable ones. Retaining only those particles which are more stable according to our indicator, we obtain a narrow elliptic ring displaying sharp edges which agrees with the nominal location of Saturn's F ring.

1 Introduction

Saturn's F ring is a fascinating narrow eccentric ring with a very rich and dynamical structure: beside its non-zero eccentricity and sharp-edges, it has multiple com-

Luis Benet
Instituto de Ciencias Físicas, Universidad Nacional Autónoma de México (UNAM)
Apdo. Postal 48–3, 62251-Cuernavaca, Mexico
e-mail: benet@fis.unam.mx

Àngel Jorba
Departament de Matemàtica Aplicada i Anàlisi, Universitat de Barcelona
Gran Via 585, 08007 Barcelona, Spain
e-mail: angel@maia.ub.es

ponents entangled in a complicated way which show a variety of short-time features Esposito (2006); Charnoz et al. (2009). This ring is located just outside the main rings of Saturn, close to Roche's limit for ice, and it is believed to be the result of the action of accretion and disruptive process Charnoz et al. (2009). Aside from the difficult questions related to its origin and evolution, its location and its highly dynamical structural properties pose interesting questions. The current understanding on the confinement of narrow planetary rings is based on the shepherd theory, introduced by Goldreich and Tremaine (1979). In its original form, the shepherd theory postulates the existence of two moons orbiting the central planet, the shepherd moons. These moons repel away the ring particles through gravitational angular-momentum exchange mechanisms, and induce ring-particle eccentric orbits which are circularised by mutual ring-particle collisions. The ring is confined between the shepherd moons where the angular-momentum torques balance, or by mean-motion resonances. While the shepherd theory is successful for the ε ring of Uranus, its application to Saturn's F ring is not so straightforward, since there is no mean-motion resonance that confines the ring, the masses of the shepherds moons Prometheus and Pandora are too small, and the angular momentum torques are not balanced at the actual location of the ring (see e.g. Esposito, 2006). In addition, the eccentricity of the ring and its sharp edges pose further questions. The confinement of Saturn's F-ring remains unexplained.

In this paper we discuss a model to understand from a dynamical point of view the confinement of Saturn's F ring. We argue that a minimal model for Saturn's F ring needs to include at least the gravitational interactions of Saturn (we also include corrections due to its flattening), the shepherd moons, and Saturn's most massive moon, Titan. We follow the scattering approach to narrow rings (Merlo and Benet, 2007) where ring particles are treated within a particle-independent model, i.e., ring particle collisions are neglected. In this approach, the location and structure of the ring follows from an ensemble of ring particles that remains trapped despite the existence of escaping and leaking mechanisms in the system, which in the present case are mainly physical collisions with the shepherd moons. We compute the orbits of an ensemble of non-interacting test particles during 3.2×10^6 periods of innermost shepherd moon, Prometheus. Test particles that remain trapped between the orbits of the shepherds are filtered with respect to a dimensionless stability index which we use as a dynamical indicator for the possibility of escape. After this filtering, we obtain a narrow eccentric ring that displays sharp edges, located close to the nominal observations for Saturn's F ring.

The paper is organized as follows: In section 2 we introduce and motivate the $(4+1)$-body problem considered as a model for the F ring of Saturn. Section 3 describes some of our numerical simulations, including the definition of the stability index and the motivation for filtering out the particles whose associated dynamical indicator is too large. Finally, section 4 summarizes the main results of the paper.

2 A 'minimalist' model for Saturn's F ring

A complete description of the dynamics of Saturn's F ring includes the gravitational interactions of Saturn with its flattening, its major moons including the influence of the shepherd moons Prometheus and Pandora, and the interactions among the ring particles themselves. The latter involves non-trivial processes associated to physical collisions among the particles of the ring, such as accretion and fragmentation processes. Clearly, the understanding of such a system is a monumental task. Here we shall thus address a simpler problem which is the understanding of a possible mechanism for confinement of Saturn's F ring and, once this is settled, we shall consider the structural properties of the resulting confined ring.

The starting point of our model is the assumption that the F ring consists of an ensemble of non-interacting test particles, which are dynamically trapped by their interactions with Saturn and its major moons. We study the dynamics of an ensemble of test particles defined by its initial conditions in phase space; their time evolution determines whether a test particle remains dynamically trapped and hence belongs to the ring, or if it simply escapes. This is the framework of the so-called scattering approach to narrow rings (Benet and Seligman, 2000; Merlo and Benet, 2007). The crude assumption of considering non-interacting test particles allows us to treat each particle independently. This assumption is therefore equivalent to disregard any effects related to collisions among the ring particles and the dynamical effects related to their actual shape and size, processes that are important for the detailed understanding of the fine structure and life-time of the ring (Poulet et al., 2000; Murray et al., 2008; Charnoz et al., 2009). In addition, we shall neglect the influence of the whole ring in the motion of any of the major bodies considered or of the particles of the ring; this is tantamount of having massless test particles. We shall assume for simplicity that the motion of all bodies takes place on the equatorial plane of Saturn. These assumptions allow us to consider a planar restricted $(N+1)$-body problem, where one test particle is influenced by the motion of N massive bodies including Saturn and its flattening, but does not influence the motion of the latter.

Our model is naturally divided into two parts. First, the motion of the N-interacting massive bodies is given in an inertial frame by the many-body Hamiltonian

$$\mathscr{H}_N = \sum_{i=0}^{N-1} \frac{1}{2m_i}(P_{x_i}^2 + P_{y_i}^2) - \sum_{i=1}^{N-1} \frac{\mathscr{G} m_0 m_i}{R_{i,0}} \left(1 + \frac{J_2}{2}\frac{R_S^2}{R_{i,0}^2}\right) - \sum_{1\le i<j}^{N-1} \frac{\mathscr{G} m_i m_j}{R_{i,j}}. \qquad (1)$$

Here, $\mathscr{G}$ denotes the gravitational constant, $m_0 = M_S = 5.68319 \times 10^{26}\,\mathrm{kg}$ (Jacobson et al., 2006) is Saturn's mass, $R_S = 60268.0\,\mathrm{km}$ (Seidelmann et al., 2007) denotes its equatorial radius, and $J_2 = 16290.71 \times 10^{-6}$ is the value of first zonal gravitational coefficient (Jacobson et al., 2006). The latter is included since we are interested in somewhat long-time integrations; higher-order terms related to the flattening are ignored since they do not provide further physical insight and simply slow down significantly the numerical calculations. The mass of the i-th body is denoted by m_i,

its position from the origin (which is the center of mass of N-body problem) by $\mathbf{R}_i$, and its momentum by $\mathbf{P}_i$. Then, $R_{i,j} = |\mathbf{R}_i - \mathbf{R}_j|$ denotes the distance between the i-th and the j-th bodies, with the convention that $i = 0$ represents Saturn, and the moons included in the model are ordered increasingly with respect to their semi-major axis.

The second part of the model is related to the motion of the test particles, whose Hamiltonian reads

$$\mathscr{H}_{\mathrm{rp}}(t) = \frac{1}{2}(p_x^2 + p_y^2) - \frac{\mathscr{G}m_0}{r_0(t)}\left(1 + \frac{J_2}{2}\frac{R_S^2}{r_0^2(t)}\right) - \sum_{i=1}^{N-1}\frac{\mathscr{G}m_i}{r_i(t)}, \tag{2}$$

where $r_i(t) = |\mathbf{r} - \mathbf{R}_i(t)|$ denotes the distance from the test particle to the i-th massive object, $\mathbf{r}$ denotes the position of the ring particle and $\mathbf{p}$ its momentum. Notice the explicit appearance of time in the test-particle Hamiltonian through the positions $\mathbf{R}_i(t)$; hence, the energy of the test particle is not a constant of motion.

What massive bodies shall we include in a simple model for the F ring? Clearly, we must include the shepherd moons Prometheus and Pandora ($m_1 = 2.4 \times 10^{-10} M_S$, $a_1 = 2.312 R_S$, $e_1 = 0.0024$; $m_2 = 2.3 \times 10^{-10} M_S$, $a_2 = 2.352 R_S$, $e_2 = 0.0042$), which are known to influence the dynamics of the ring, though they do not confine it completely (see Esposito, 2006). The resulting $(3+1)$-body model defined by Saturn, the shepherd moons and the test particle, yields a broad ring instead of a narrow one, which spans essentially all the available initial condition space between the orbits of the shepherd moons. This follows from the fact that the masses of shepherd moons are exceedingly small, so their influence on the test particles is essentially local: Test particles either collide with them, or essentially do not feel their influence at all; their motion is a precessing Kepler ellipse which is too weakly perturbed by the shepherds. Therefore, our minimalist model must include at least another moon, thus becoming a planar restricted $(4+1)$-body problem.

There is no obvious choice for such a third moon in the model, since there is no resonance that actually confines the ring (Esposito, 2006). Two possible options are Titan and Mimas: Titan is the most massive moon of Saturn's satellite system ($M_{\mathrm{Titan}} = 2.3669 \times 10^{-4} M_S$), with a nominal eccentricity of $e_{\mathrm{Titan}} = 0.0288$, but it is located rather far away from the ring, $a_{\mathrm{Titan}} = 20.27 R_S$. In turn, Mimas is the major moon of Saturn closest to the F ring ($a_{\mathrm{Mimas}} = 3.076 R_S$) and may play an important role, since Pandora is close to a $3:2$ co-rotation eccentric resonance with Mimas (French et al., 2003). Yet, the mass of Mimas is comparatively small, $M_{\mathrm{Mimas}} = 6.6 \times 10^{-8} M_S$. We notice that the ratio of the force exerted by Titan on a test particle at the nominal semi-major axis of the F ring ($a_{\mathrm{Fring}} = 2.324 R_S$) is ~ 4 times larger than the force exerted by Mimas, when Titan is at its furthest location from the particle and Mimas is at the closest one. For this reason we shall consider in our model the influence of Titan on a precessing Kepler eccentric elliptic orbit. Finally, due to the small mass ratio between Titan and Saturn and the shepherds and Titan, we simplify the numerics by computing the precessing Kepler motion of Titan due to the gravitational attraction of Saturn and its J_2 coefficient, and for the shepherds we include the additional perturbations by Titan; we further consider that Saturn remains at the origin.

We are interested in the existence of regions of trapped motion between the orbits of the two shepherd moons. Note that our model can be seen as a central field (with a central oblate mass) under a time dependent perturbation coming from the motion of the moons and Saturn. If the motion of these bodies (described by Hamiltonian (1)) is quasi-periodic, then the time dependent perturbation that appears in Hamiltonian (2) is also quasi-periodic. This means that, if all these peturbations are small enough and some generic conditions hold, a version of the KAM theorem (Jorba and Simó, 1996; Jorba and Villanueva, 1997) can be used to ensure the existence of plenty of quasi-periodic motions for a particle between the two shepherd moons. As these conditions are very difficult to check in this model, we will use numerical simulations to study the dynamics of a test particle.

Therefore, let us define the conditions for escape: We consider that a test particle escapes if it leaves the region defined by the orbits of the shepherds, i.e., if it is not located within the region defined by innermost radial position of Prometheus' orbit and the outermost of Pandora's. In addition, a test particle is said to collide if it is located within Hill's radius of a shepherd moon, that is, $r_i < R_{H_i} = a_i(m_i/3m_0)^{1/3}$ (with $i = 1,2$ for Prometheus and Pandora respectively). In this case, the test particle will be treated as an escaping particle, since such an event corresponds to a physical collision with one of the shepherds (Ohtsuki, 1993). In either case, the integration of the orbit shall be terminated and the test particle is disregarded. On the other hand, if the test particle does not fulfill any of these requirements before the end of the numerical integration at t_{end}, the test particle is considered to be trapped and, in that sense, a particle of the ring. We shall see below that an additional criterion related to the stability properties of the orbits and the possibility to escape must be imposed.

In the following, mass units shall be expressed in terms of Saturn's mass M_S, distances in terms Saturn's equatorial radius R_S, and time is given in terms of $T_{\text{Prom}} = T_1 = 2\pi$, which corresponds to a full Kepler period of Prometheus.

3 Numerical results

A dynamical problem is fully defined once the initial conditions are set. Since we are interested in the dynamics of the test particles, we shall fix the initial conditions of the massive bodies, and consider a region of the phase space for the test particles; different initial conditions correspond to independent test particles. The initial conditions of the test particles are defined by the initial semi-major axis a, the eccentricity e, and two angles defining the initial orientation of the instantaneous precessing ellipse ω, the argument of pericenter, and the position along the ellipse ϕ, the true anomaly. In the following we shall focus in the phase-space region defined by $a \in [2.318\,R_S, 2.345\,R_S]$, $e \in [0, 0.00145]$ and $\phi, \omega \in [-\pi, \pi]$. We note that this region in phase space, after projection into the coordinate space, spans the (planar) region between the orbits of Prometheus and Pandora. Therefore, this region includes the orbital elements compatible to particles belonging to Saturn's F ring, but is not restricted to those orbital elements only.

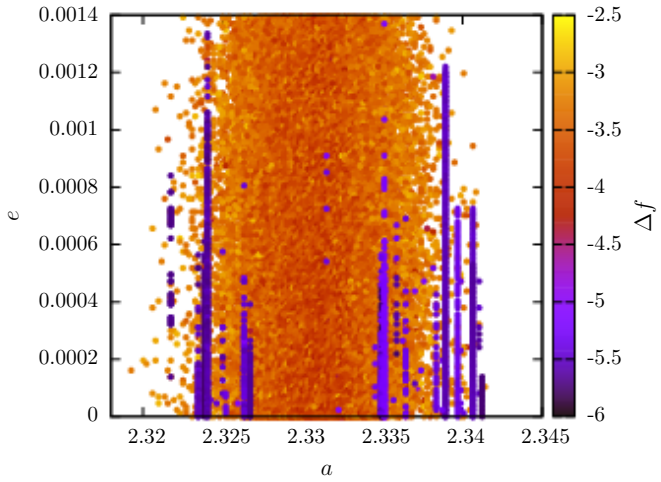

Fig. 1 Projection into the semi-major axis vs eccentricity plane of the initial conditions of test particles that remain trapped at least for $t_{\text{end}} = 2.4 \times 10^6 T_1$. The color code is the stability index Δf in logarithmic scale associated to the mean motion. Notice that there are two localized regions where the particles exhibit an enhancement of the stability index (blue stripes).

The numerical results presented below have been computed using a high-order Taylor's method (maximum order of the Taylor expansion is 28) for the numerical integration; see Jorba and Zou (2005) for details on the method. The accuracy of the integrations is such that the energy and the angular momentum of Titan's Kepler motion is conserved to machine precision throughout the integration.

Figure 1 shows the projection into the initial semi-major axis a and eccentricity e plane of test particles that remain trapped at least for $t_{\text{end}} = 2.4 \times 10^6$ periods of Prometheus. In these simulations, the orientation of the initial Kepler ellipses was varied considering 10 equally spaced values, while the true anomaly was set to 0; the semi-major axis and the eccentricity were set on a grid of 256 points for each value of ω. The results in Fig. 1 show that the particles that remain trapped still form a wide and seemingly connected region of both a and e. The result seems deceiving: While the inclusion of Titan in the model foments further collisions with the shepherds, it does not yield a narrow ring that could be compared with the observations, at least after the end of the integration considered. However, contrary to the $(3+1)$-body model (the shepherd moons and Saturn), in the present case the trapped test particles do not *a priori* move along essentially stable precessing Kepler ellipses, due to the presence of Titan. Indeed, since the motion of Titan is eccentric, there is no conserved quantity similar to the Jacobi integral in the circular restricted three-body problem. Then, the eccentric motion of Titan allows test particles to explore radially more extended regions, and thus allows them to fulfill one conditions to escape. As we shall see below, some test particles happen to explore radially more extended regions than others; we shall argue that these are particles that eventually escape.

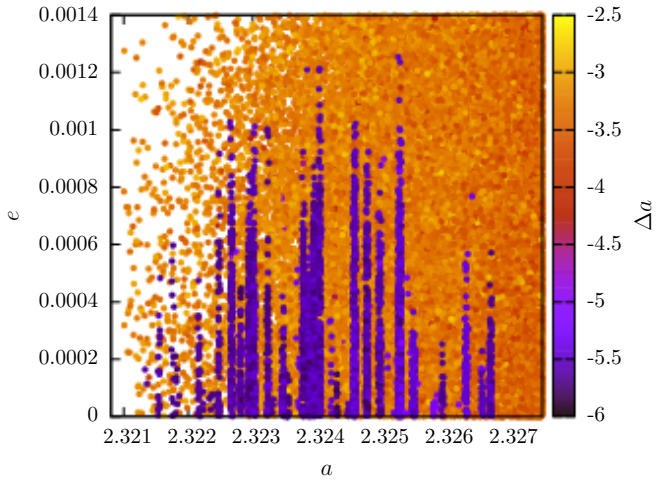

Fig. 2 Same as Fig. 1 for test particles that remain trapped at least for $t_{\rm end} = 3.2 \times 10^6 T_1$ close to the observed semi-major axis for Saturn's F ring. In this case, the color code corresponds to base-10 logarithm of the stability index Δa constructed with respect to the mean semi-major axis.

It is in this sense that we address the stability properties of the test particles that remain trapped, and consider a frequency type analysis Laskar (1992, 1993). More specifically, motivated from the fact that the motion of the test particle is a small perturbation from an integrable system (the Kepler problem with flattening), we study the stability index defined by the ratio of the standard deviation of a frequency and its average value, computed along the whole trajectory; in particular, we consider the stability index associated to the mean motion $\Delta f = \sigma_f / \overline{f}$. In terms of Δf, quasi-periodic motion yields $\Delta f = 0$; hence, non-zero values of Δf indicate a departure from stable (quasi-periodic) motion.

From the numerical integration of the orbits, we compute the main frequencies of the motion every 200 revolutions of Prometheus using a collocation method (Gómez, Mondelo, Simó, 2010), from which $\overline{f}$ and σ_f are calculated whenever the test particle remains trapped. The color code in Fig. 1 is based on $\log_{10}(\Delta f)$. Figure 1 displays some vertical blue-violet stripes localized around $a \sim 2.324$ and $a \sim 2.340$, where the particles exhibit an enhancement of the stability index ($\Delta f \sim 10^{-5}$) in comparison to the rest of the trapped particles, i.e. roughly two orders of magnitude. Interestingly, the first group of blue-violet stripes quoted above lies close to the nominal semi-major axis of Saturn's F ring; Fig. 2 displays more extended ($t_{\rm end} = 3.2 \times 10^6 T_1$) and detailed simulations focusing on this region, where the initial angles of the test particles are chosen at random. The logarithmic color code in Fig. 2 is defined now through the stability index Δa associated to the mean semi-major axis of the orbit (during 200 revolutions of Prometheus), which is a measure of the radial excursion performed by test particles up to $t_{\rm end}$.

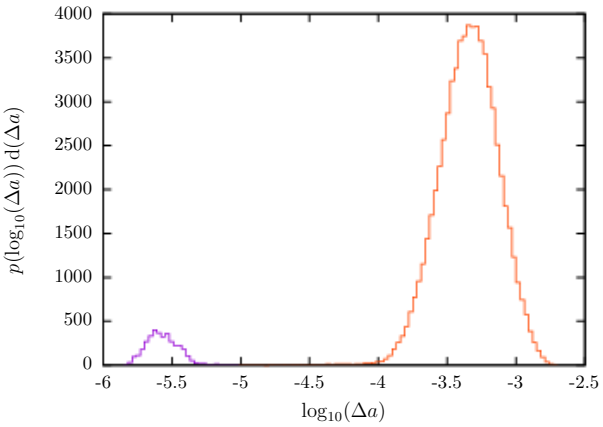

Fig. 3 Frequency histogram of $\log_{10}(\Delta a)$ for the data used for Fig. 2; the normalization corresponds to the total number of trapped test particles. Note that Δa is clearly separated in two disjoint ranges.

Groups of localized (blue-violet) stripes can again be distinguished in Fig. 2 among the trapped orbits; our simulations suggest that there is no particular, or only a weak dependence, on the initial angles for these test particles. We observe that according to the stability index Δa, the trapped test particles display two well-separated scales, which correspond to radial excursions of few kilometers and few hundreds of kilometers. This is illustrated in Fig. 3 where we show the frequency histogram of $\log_{10}(\Delta a)$ for the data used in Fig. 2.

We interpret the results of Fig. 3 as follows: A test particle moves along a perturbed precessing ellipse; the orbit displays an additional but quite limited radial excursion due to Titan's interaction. Titan's eccentric orbit may create conditions which permit, in a rather short-time scale, an abrupt change in the semi-major axis and eccentricity, which in turn results in more extended radial excursion of the orbit. This increment of the radial excursion may provide eventually the conditions for the escape of the test particle; in our simulations, this corresponds typically to a collision with one of the shepherd moons. Test particles that experience these events but are still trapped at time t_{end} are those that correspond to the orange–yellow points in Figs. 1 and 2. The blue-violet dots correspond to test particles that may have experienced very few or even none abrupt changes in their semi-major and eccentricity values; therefore, the associated value of Δa is very small.

According to this interpretation, it is a question of time that the test particles belonging to the orange–yellow region will eventually escape. Note that this does not exclude that test particles with very small values of Δa finally escape, but suggests that the time required may be comparatively longer. The structure of Fig. 3 suggests to filter the trapped test particles according to the stability index, and retain only those particles whose stability index is small enough. In particular, we shall consider as ring particles those that satisfy the criterion $\Delta a < 10^{-5}$.

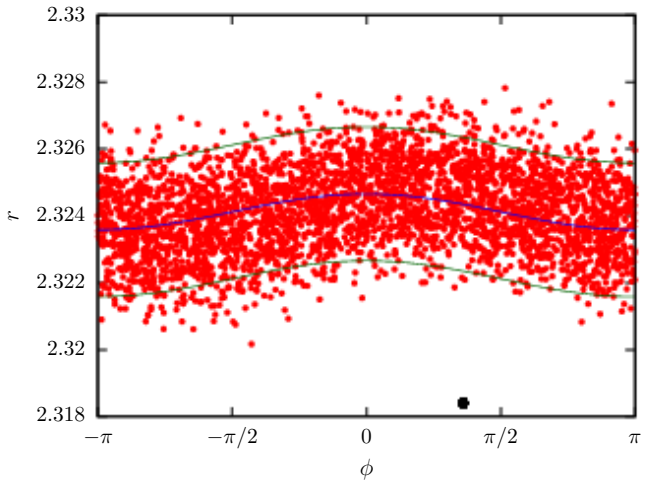

Fig. 4 Snapshot of the ring particles after filtering near the end of our simulations. The x-axis is the azimuthal angle, and the y-axis is the radial location. The blue middle line represents the best-fit of the particles of the ring to a Keplerian ellipse; the outer lines correspond the same ellipse shifted upwards or downwards by $0.002\,R_S$ and serve to obtain a rough estimate of the width of the ring. The black dot close to the bottom-right of the figure is Prometheus.

Using this filtering, we present in Fig. 4 a snapshot of the ring obtained close to the nominal location of Saturn's F ring. The ring is clearly narrow, eccentric and displays sharp edges. Fitting a Keplerian ellipse to the data used in Fig. 4 we obtain estimates for the semi-major axis $a_{\rm fit} \approx 2.3241\,R_S$ and the eccentricity $e_{\rm fit} \approx 2.32 \times 10^{-4}$. A rough estimate for the width of the ring is obtained by shifting radially this Keplerian ellipse; we obtain that within a width $\delta r \lesssim 0.005\,R_S \approx 300\,$km contains more than 90% of the ring particles. There is indeed a remarkable correspondence of these values with the observations for Saturn's F ring. Yet, we must emphasize that this *a posteriori* consistency check of comparing our results with the observational data is not a proof of the dynamical consistency of the filtering; only longer numerical integrations, which are quite time consuming, can prove or disprove if the filtered test particles indeed escape. With this proviso, the result is quite rewarding.

4 Discussion

In this paper, we have introduced a simple $(4+1)$-body model for Saturn's F ring, consisting of four bodies (Saturn, Prometheus, Pandora and Titan) which influence the dynamics of a massless test-particle. The model includes the flattening of Saturn through its second zonal coefficient J_2. We argue that a realistic model for the understanding of the confinement and stability of Saturn's F ring requires at least include these interactions. We found that after long integration times ($t_{\rm end} = 3.2 \times 10^6 T_1$)

there is a wide region in the initial conditions plane (a vs e, essentially independent of the initial angles) which remain trapped. These test particles show a separation of scales (about two orders of magnitude) with respect to a stability index defined as the ratio Δf of the standard deviation of the mean-motion frequency to its average value; the frequencies are computed during a fixed interval of time $200T_1$ and the average is performed including all the orbital data. Similar results are obtained for a related indicator Δa, defined on the mean semi-major axis, which is a measure of the radial excursion of the orbit of the test particle during the integration time. In the initial condition plane, the regions of enhanced stability appear as localized stripes immersed in a wide region of trapped test particles.

We have argued that test particles with larger values of Δf or Δa eventually escape from the neighborhood of the ring, or simply collide with one of the shepherds. By filtering out those test particles which are not too stable according to the stability index, we end up with a set of particles that form a narrow ring in the vicinity of the observed Saturn's F ring. Beside being narrow, the ring obtained is eccentric and displays sharp edges. Our estimates for the semi-major axis, eccentricity and width of the ring agree with the observational data. Although the filtering has to be further validated by longer integrations of the orbits, we claim that this model including the stability with respect to escapes may help to understand the confinement of Saturn's F ring as well as some of its structural properties. The basic dynamical mechanism is related to the existence of invariant structures of the dynamics which build transport barriers that effectively trap and confine the particles of the ring; test particles that in our simulations remain trapped but do not survive the filtering procedure, are particles whose dynamics is very slowly drifting away by exploring radially more extended regions, until they eventually collide with one of the shepherd moons. Note that this mechanism explains dynamically the confinement of Saturn's F ring: the organizing object which gives rise to the confining invariant structures explains the observed semi-major axis and eccentricity; the invariant structures which are barriers for the ring particles explain the sharp edges observed in the ring.

Acknowledgements This work was initiated during LB's sabbatical year at the Universitat de Barcelona, which was partially supported by DGAPA (UNAM) and Min. Educación (SAB2010-0123, Spain). We acknowledge financial support provided by the projects IN–110110 (DGAPA–UNAM), 79988 and 144684 (CONACyT), 334309729-9729-4-9 (Min. Ciencia e Innovación), MTM2009-09723 (Min. Ciencia e Innovación) and 2009 SGR 67 (Generalitat de Catalunya). It is a pleasure to thank Carles Simó for his encouragement, valuable comments, questions and discussions.

References

Benet, L., Seligman, T. H.: 2000, "Generic occurrence of rings in rotating scattering systems", Phys. Lett. A **273**, 331–337.

Charnoz, S., Dones, L., Esposito, L.W., Estrada, P.R., Hedman, M.M.: Origin and evolution of Saturn's ring system. In: Dougherty, M.K., Esposito, L.W., Krim-

igis, S.M. (eds.), Saturn from Cassini-Huygens, pp 537-575. Springer, Dordrecht (2009).

Esposito, L. W.: Planetary rings. Cambridge University Press, Cambridge (2006).

French, R.G., McGhee, C.A., Dones, L., Lissauer, J.J.: 2003, "Saturn's wayward shepherds: the peregrinations of Prometheus and Pandora", Icarus **162**, 143-160.

Goldreich, P., Tremaine, S. D.: 1979, "Towards a theory for the Uranian rings", Nature **277**, 97–99.

Gómez, G., Mondelo, J.M., Simó, C.: 2010, "A collocation method for the numerical Fourier analysis of quasiperiodic functions I: Numerical tests and examples", DCDS-Series B **14**, 41-74.

Jacobson, R.A., et al.: 2006, "The Gravity Field of the Saturnian System from Satellite Observations and Spacecraft Tracking Data", Astronm. J. 132, 2520 (2006).

Jorba, À., Simó, C.: 1996, "On quasiperiodic perturbations of elliptic equilibrium points", *SIAM J. Math. Anal.* **27**, 1704–1737.

Jorba, À., Villanueva, J.: 1997, "On the persistence of lower dimensional invariant tori under quasi-periodic perturbations", *J. Nonlinear Sci.* **7**, 427–473.

Jorba, À., Zou, M.: 2005, "A software package for the numerical integration of ODE by means of high-order Taylor methods", Experiment. Math. **14**, 99-117.

Laskar, J.: 1992, "The chaotic behavior of the solar system: a numerical estimate of the chaotic zones", Icarus **88**, 266-291.

Laskar, J.: Introduction to frequency map analysis. In: Simó, C. (ed) Hamiltonian Systems With Three or More Degrees of Freedom, NATO Adv. Sci. Inst. Ser. C Math. Phys. Sci., vol 533, pp. 134-150. Kluwer Acad. Publ., Dordrecht, (1999).

Merlo, O., Benet, L.: 2007, "Strands and braids in narrow planetary rings: A scattering system approach", Celest. Mech. Dyn. Astr. **97**, 49-72.

Murray, C.D., Beurle, K., Cooper, N.J., Evans, M.W., Williams G.A., Charnoz, S.: 2008, "The determination of the structure of Saturn's F ring by neraby moonlets", Nature **453**, 739-744.

Ohtsuki, K.:1993, "Capture probability of colliding planetesimals - Dynamical constraints on accretion of planets, satellites, and ring particles", Icarus **106**, 228-246.

Poulet, F., Sicardy, B., Nicholson, P.D., Karkoschka, E., Caldwell, J.: 2000, "Saturn's ring-plane crossings of August and November 1995: A model for the new F-ring objects", Icarus **144**, 135-148.

Seidelmann, P.K., et al.: 2007, "Report of the IAU/IAG Working Group on cartographic coordinates and rotational elements: 2006", Celest. Mech. Dyn. Astr. **98**, 155-180.